Pattern-Reconfigurable Yagi–Uda Antenna Based on Liquid Metal

Jiaxiang Hao, Jian Ren, *Member, IEEE*, Xiaoyu Du, Jan Hvolgaard Mikkelsen, Ming Shen, and Ying Zeng Yin, *Member, IEEE*

***Abstract*—A pattern-reconfigurable Yagi–Uda antenna based on liquid metal is presented. The antenna consists of a balun-fed active dipole and a pair of stretchable passive parasitic dipoles, which are implemented by eutectic gallium-indium (EGaIn) alloy embedded in microfluidic channels. The parasitic dipoles are driven at each end by two low-cost, three-dimensional printed media rods. Afterward, spinning the rods at different angles leads to varying degrees of stretching upon the stretchable dipoles. Note the length of passive parasitic dipoles is a vital factor for antenna radiation reconfiguration. The antenna exhibits bidirectional radiation if the parasitic dipoles are equal in length. Otherwise, directional radiation toward the shorter parasitic dipole direction can be obtained. Based on the above-mentioned working principle, a pattern-reconfigurable antenna working in wireless local area network (WLAN) band is fabricated and measured. Apart from the reconfigurable capability, the proposed antenna keeps operating in the WLAN band of 2.4–2.48 GHz during the whole shape deformation.**

***Index Terms*—3-D printing, bidirectional radiation, directional radiation, Ecoflex elastomer, liquid metal, microfluidic channels, pattern-reconfigurable, Yagi–Uda antenna.**

I. Introduction

RECONFIGURABLE antennas, being able to meet the increasing demands in communication systems with diverse functions, have become a hotspot [1]–[4]. According to the capability, reconfigurable antennas can be roughly classified into frequency-reconfigurable antennas [1], polarization-reconfigurable antennas [2], pattern-reconfigurable antennas [3], and hybrid reconfigurable antennas [4]. Among them, by switching state to desired radiation pattern, pattern-reconfigurable antenna has gained continuous attention. However, traditional rigid metal antennas used in wireless communication systems are suffering several limitations in terms of elasticity and toughness. With fixed antenna shapes, any deformation like bending, meandering, and folding, would cause a deterioration in performance. In [5], The eutectic gallium-indium (EGaIn) alloy, a kind of liquid metal at room temperature, was first applied for liquid metal antennas. This new type of alloy material with many novel material properties, provides a promising prospect for interdisciplinary research for reconfigurable antenna designs [6]–[8]. By stretching the flexible material, a frequency-reconfigurable antenna in [5] can be obtained according to the varying length of the dipole made of EGaIn alloy. Though excellent electrical properties of EGaIn alloy has been verified in [6], excitation directly upon this alloy could still lead a possibility of leakage of liquid. In this situation, coupling feed [9]–[11] as well as excitation upon rigid part of antennas [12]–[15] can effectively avoid that possibility. Both solutions either suffer the complexity of precisely continuous control or residue after times of pushing/withdrawing of liquid metal. Therefore, fulfilling microfluidic channels in a fully enclosed flexible carrier with liquid metal has been studied and researched. Flexible materials like Kapton polyimide [16], benzocyclobutene (BCB) [17], Ecoflex [18], and polydimethylsiloxane (PDMS) [19], are widely used in reconfigurable antenna designs [20]–[25]. Most of those antennas are naturally wideband. Reconfigurable characteristics realized by deformation in antenna shapes could also lead to a deviation of operating band.

In this letter, a pattern-reconfigurable antenna based on liquid metal is presented, as shown in Fig. 1. The dipole is fed by a balun, while the two parasitic dipoles made of liquid metal are coupled aside. Then, the possibility of the leakage of liquid metal as well as the unstable port match can be avoided. Also, a platinum-catalyzed silicone elastomer (EcoFlex) is applied for

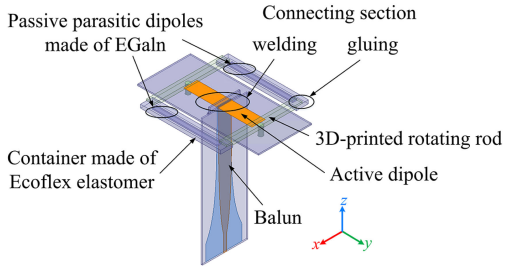

Fig. 1. Layout of pattern-reconfigurable Yagi–Uda antenna.

Manuscript received December 31, 2020; accepted February 1, 2021. Date of publication February 9, 2021; date of current version April 7, 2021. This work was supported in part by the National Natural Science Foundation of China under Grant 61901316 and 62071351; in part by the 111 Project of China; and in part by the Open Project of the State Key Laboratory of Millimeter Waves, Southeast University, under Grant K202102. *(Corresponding author: Jian Ren.)*

Jiaxiang Hao, Xiaoyu Du, and Ying Zeng Yin are with the National Key Laboratory of Antennas and Microwave Technology, Xidian University, Xi'an 710071, China (e-mail: hjx1996china@outlook.com; duxiaoyu0101@163.com; yyzeng@mail.xidian.edu.cn).

Jian Ren is with the National Key Laboratory of Antennas and Microwave Technology, Xidian University, Xi'an 710071, China, and also with the State Key Laboratory of Millimeter Waves, Southeast University, Nanjing 210096, China (e-mail: renjian@xidian.edu.cn).

Jan Hvolgaard Mikkelsen and Ming Shen are with the Antennas, Propagation, and Radio Networking Section, Department of Electronic Systems, Faculty of Engineering and Science, Aalborg University, Aalborg 9220, Denmark (e-mail: jhm@es.aau.dk; mish@es.aau.dk).

Digital Object Identifier 10.1109/LAWP.2021.3058115

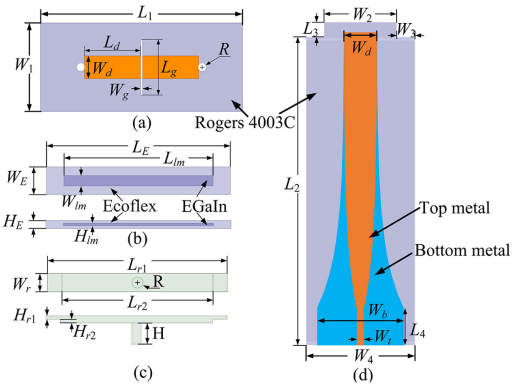

Fig. 2. Details of each part of the antenna. (a) Dipole substrate, a gap in the center for connecting with balun substrate, two penetrated holes aside for fixing rotating rods. (b) Balun substrate, a gradient line from a width of characteristic impedance of 50 Ω to active dipole width. (c) Flexible parasitic dipoles with liquid metal sealed in its microfluidic channels. (d) Rotating rod (3-D printed) for driving Ecoflex elastomer.

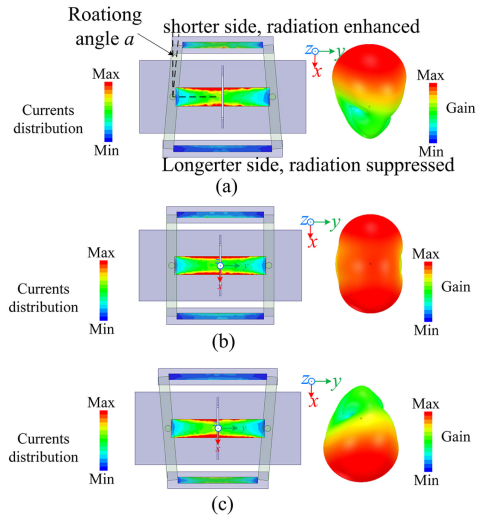

Fig. 3. Simulated currents distribution on the dipoles and its 3-D radiation patterns for different rotating angle. (a) $a = 5°$, (b) $a = 0°$, and (c) $a = -5°$.

making flexible containers. The ability to vary the length of those parasitic dipoles renders the proposed antenna a pattern-reconfigurable radiation characteristic. The realization of this characteristic is quite simple: When the parasitic dipoles are equal in length, the antenna exhibits bidirectional radiation. By stretching one dipole but shortening the other one, the radiation would be enhanced along the shortened dipole's direction, while the radiation toward longer side suppressed. Therefore, the antenna switches to a directional radiation state. Also, the shape deformation caused by switching action would not deviate antenna from the preset WLAN band.

II. Antenna Design

A. Antenna Configuration

The antenna topology and all details of each part are shown in Figs. 1 and 2. The presented antenna contains following parts: 1) a printed active dipole; 2) a pair of passive parasitic dipoles; 3) two media rotating rods for motivating; and 4) a feeding balun. The active dipole and its balun are fabricated, respectively, on two different Rogers 4003C ($\varepsilon_r = 3.55$, $\tan\delta = 0.0027$) substrates with a thickness of 0.813 mm. Meanwhile, a longitudinal slot and a pair of holes are etched on the dipole substrate to mount the balun for their connection and fix a pair of rotating rods, separately. Those 3-D printed rods are not only reliable in structure but also cheap in price. Besides, the passive parasitic dipoles are made of liquid metal alloy of 75% gallium, 25% indium (EGaIn) with a melting point of 15.5°C and a conductivity of 3.4×10^6 S/m [5]. Thus, the fluidity of the alloy in room temperature enables it to flow with the deformation of the microfluidic channels fabricated by Ecoflex elastomer ($\varepsilon_r = 2.3$, loss $\tan\delta = 0.027$) [17]. The channel fabrication process will be discussed in Section III.

B. Pattern-Reconfigurable Principle

The pattern radiation reconfigurable function is realized under the working principle of the Yagi–Uda antenna. As depicted in [26], the antenna is composed of a fed dipole, a reflector lightly longer than the fed dipole, and several directors slightly shorter than the fed dipole. The length of the passive elements and their position relative to that fed dipole are vital to the antenna radiation pattern. On the one hand, the passive element with marginally longer length can act as a reflector and hence suppress the radiation of the dipole in its direction. On the other hand, the radiation of the dipole can be enhanced toward a slightly shorter element post in the opposite direction. Thus, by changing the length of those parasitic dipoles, the pattern radiation pattern of the antenna can be changed.

To specifically explain above radiation characteristic, an antenna designed to work at 2.45 GHz has been simulated in professional full-wave simulation software ANSYS HFSS. As shown in Fig. 3, spinning the two rotating rods at opposite angles reduces the length of the flexible parasitic dipole on one side but increases the other one on the opposite. Accordingly, the microfluidic channel and the liquid metal strip of each side follow the identical changing trend as the corresponding parasitic dipoles. Obviously, the currents on the shorter side are stronger than that on the longer side. Therefore, directional radiation can be observed when the parasitic dipoles are different in length. In contrast, the pattern would switch to bidirectional radiation when the parasitic dipoles are equal.

III. Experiment Validation

To verify the above reconfigurable characteristic, an antenna applied for WLAN band (2.4–2.48 GHz) has been designed, fabricated, and measured. As far as possible to obtain a maximum front-to-back ratio at directional radiation state, under the condition of operating band within WLAN band during the whole shape deformation, the antenna has been optimized in the software of HFSS. Thus a maximum rotation angle of $a = \pm5°$ has been decided. At the maximum rotation angle, the channel on one side is stretched to 47.3 mm and the other side stretched to 38.6 mm. Therefore, the working tuning range of the

TABLE I
DIMENSIONS OF THE ANTENNA IN (mm)

Parameters	W_d	L_d	W_g	L_g	W_1	L_1	W_t	H_{r1}	L_E
Value	9	22.2	0.813	22	35	80	1.9	1	53
Parameters	W_3	L_3	W_4	L_4	W_2	L_2	W_b	H_{r2}	R
Value	5	3.8	30	10	20	84	24	1	1.5
Parameters	W_{lm}	L_{lm}	H_E	H_{lm}	L_{r1}	L_{r2}	W_r	W_E	
Value	3	43	2.25	0.75	50	42	5	8	

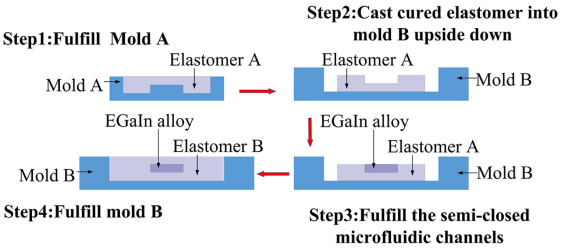

Fig. 4. Fabrication process of stretchable microfluidic channel.

microfluidic channel is 38.6 to 47.3 mm. All the final parameters of the antenna are listed in Table I.

A. Fabrication Process

In this letter, the proposed reconfigurable pattern radiation is realized by changing the length of the parasitic dipoles. Those parasitic dipoles are bonded to rotating rods by super glues. The active dipole and balun are connected by welding at their joint point. They can be prepared following standard PCB fabrication process while the rotating rods and molds required for making microchannels rely on 3-D printing technology.

Fig. 4 shows the fabrication process of the microfluidic channels, specific steps are described as follows:

Step 1: Pour a 1:1 fully mixed Ecoflex A and B solution into a 3-D printed Mold A.

Step 2: Cast the cured Elastomer A into another 3-D printed Mold B upside down (the channel on top).

Step 3: Fulfill the channel in Elastomer A with EGaIn alloy.

Step 4: Fulfill Mold B with mixed Ecoflex solution.

Different from the fabrication process proposed in [19] and [24], without the help of a hotplate, we peeled the semi-closed elastomer A in step 1 and the fully enclosed elastomer B in step 4 off from Molds after a 4 h room-temperature cure. In step 2, instead of injecting the EGaIn alloy into a fully enclosed microfluid channel, the semi-closed channel is filled with this alloy in Mold B in air. When exposed in air, a thin oxide "skin" of gallium can be quickly formed by these EGaIn alloys reacting with oxygen, which can not only stop further chemical reaction but also show no significant effect on electrical transport of the alloy [6]. It is worth mentioning that in step 3 the operation of the filling must be gentle so that the alloy already in the microchannel would not be affected as the density of the solution is distinct from that of EGaIn alloy.

Depicted in Fig. 5, the antenna prototype and measured environment are illustrated. The length of the channel can be changed

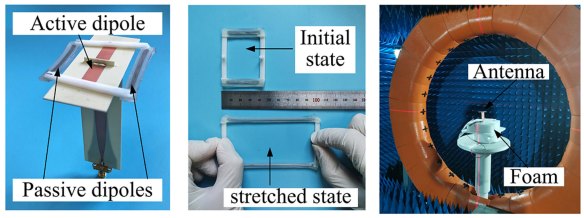

Fig. 5. (a) Overall profile of proposed antenna. (b) Flexible dipoles glued to rotating rods. (c) Measured environment.

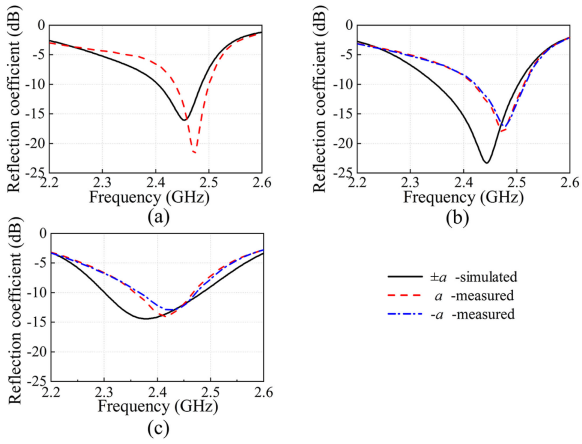

Fig. 6. Simulated and measured reflection coefficient for different rotating angle. (a) 0°, (b) ±3°, and (c) ±5°.

by stretching the elastomer. When the channel is prolonged, its width will naturally change. However, verified in software of HFSS, this change in width has little influence to the proposed antenna. It is found this flexible dipole stretched up to two times compared to its initial length suffers no severe deterioration in physical structure or its connection with rotating rods, which guarantees its stability. Moreover, the cylindrical parts of those rotating rods are similar with the holes on dipole substrate in size. Thus, when rotating the rods, the retraction of the parasitic dipoles can be ignored. The antenna can be fixed at a desired state.

B. Antenna Performance

The simulated reflection coefficient is shown in Fig. 6. Depicted in the figure, the antenna realized a −10 dB bandwidth over the WLAN band of 2.4–2.48 GHz. Moreover, the comparison of the results in Fig. 6 indicates an excellent agreement between the experiment and simulation results with a deviation of merely 0.8% (20 MHz). Furthermore, the measured and simulated gain (dBi) and efficiency (%) versus frequency in each state are shown in Fig. 7. Antenna efficiency measured in WLAN band is no less than 60% at each state.

As Fig. 8 shows, by rotating the angle of the dielectric rods on both sides from 5° to 0° and 0° to −5°, the antenna radiation pattern switches from directional radiation toward one dipole's direction to bidirectional radiation and from bidirectional radiation to directional radiation, respectively, exhibiting reasonable radiation reconfiguration ability. The simulated gain of this

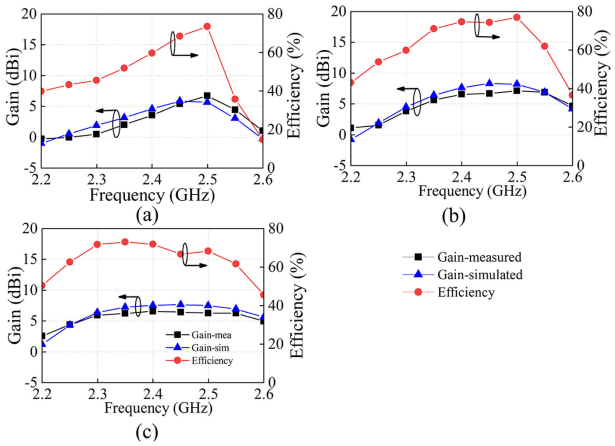

Fig. 7. Antenna efficiency and measured gain for different rotating angle. (a) 0°, (b) 3°, and (c) 5°.

TABLE II
COMPARISON OF LIQUID METAL ANTENNAS

Ref.	feeding method	possibility of leakage	Realization of reconfigurability	possibility of residue
[5]	Directly fed	Yes	stretch	No
[24]	Directly fed	Yes	blow	No
[9]	Coupling fed	No	push/withdraw	Yes
[12]	Rigid part fed	No	push/withdraw	Yes
Pro.	Balun fed	No	stretch	No

antenna at 2.45 GHz increases from 5.8 dBi at 0° to 7.8 dBi at ±5°. The antenna obtains a maximum front-to-back ratio >16 dB at this directional radiation state.

C. Discussion

In this letter, a combination of the concept of traditional Yagi–Uda antenna, the flexibility of Ecoflex material and the fluidity of the liquid metal in room temperature has been implemented to obtain a pattern-reconfigurable antenna. As shown in Table II, compared with other works, the possibility of leakage as well as residue can be avoided through applied methods. The stability and safety of this antenna can be guaranteed. Moreover, the electrical control of the proposed antenna can be realized by applying a planar dielectric elastomer actuator (DEA) [22] upon the rotating rods.

IV. CONCLUSION

A pattern-reconfigurable Yagi–Uda antenna based on liquid metal has been presented. The antenna consists of a balun-fed active dipole, a pair of passive parasitic dipoles, and two rotating rods. Different from the other works, the microfluidic channels are fabricated without furnace, along with mentioned semi-closed channel, which greatly simplifies the preparation. No drawback compared with those made by a furnace has been found. Meanwhile, the stability of the proposed antenna in practice can be guaranteed with both physical (welding) and chemical (gluing) connection in the joints of each part. By spinning the desired angle of those rotating rods, the antenna can realize a pattern-reconfigurable characteristic switching from bidirectional radiation to directional radiation. The maximum gain of proposed antenna is improved about 2.4 dBi from bidirectional to directional state. A maximum F/B ratio >16 dB at directional radiation state can be obtained.

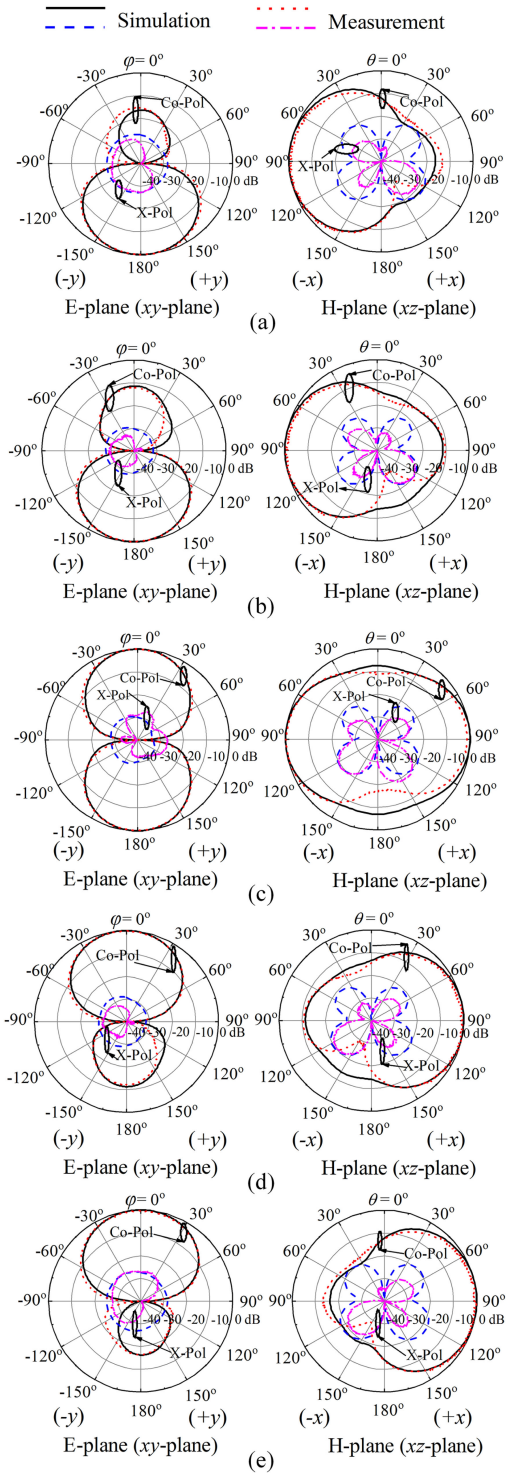

Fig. 8. Simultaed and measured radiation patterns of E-plane (*xy* plane) and H-plane (*xz* plane) for different rotating angle. (a) 5°, (b) 3°, (c) 0°, (d) −3°, and (e) −5°.

REFERENCES

[1] T. Li, H. Zhai, X. Wang, L. Li, and C. Liang, "Frequency-reconfigurable bow-tie antenna for Bluetooth, WiMAX, and WLAN applications," *IEEE Antennas Wireless Propag. Lett.*, vol. 14, pp. 171–174, 2015.

[2] A. Bhattacharjee, S. Dwari, and M. K. Mandal, "Polarization-reconfigurable compact monopole antenna with wide effective bandwidth," *IEEE Antennas Wireless Propag. Lett.*, vol. 18, no. 5, pp. 1041–1045, May 2019.

[3] J. Ouyang, Y. M. Pan, and S. Y. Zheng, "Center-fed unilateral and pattern reconfigurable planar antennas with slotted ground plane," *IEEE Trans. Antennas Propag.*, vol. 66, no. 10, pp. 5139–5149, Oct. 2018.

[4] N. Nguyen-Trong, L. Hall, and C. Fumeaux, "A frequency- and pattern-reconfigurable center-shorted microstrip antenna," *IEEE Antennas Wireless Propag. Lett.*, vol. 15, pp. 1955–1958, 2016.

[5] J.-H. So, J. Thelen, A. Qusba, G. J. Hayes, G. Lazzi, and M. D. Dickey, "Reversibly deformable and mechanically tunable fluidic antennas," *Adv. Mater.*, vol. 19, no. 22, pp. 3632–3637, Nov. 2009.

[6] M. D. Dickey, "Stretchable and soft electronics using liquid metals," *Adv. Mater.*, vol. 29, no. 27, Jul. 2017.

[7] D. Rodrigo, L. Jofre, and B. A. Cetiner, "Circular beam-steering reconfigurable antenna with liquid metal parasitics," *IEEE Trans. Antennas Propag.*, vol. 60, no. 4, pp. 1796–1802, Apr. 2012.

[8] G. J. Hayes, S. Ju-Hee, A. Qusba, M. D. Dickey, and G. Lazzi, "Flexible liquid metal alloy (EGaIn) microstrip patch antenna," *IEEE Trans. Antennas Propag.*, vol. 60, no. 5, pp. 2151–2156, May 2012.

[9] V. T. Bharambe, J. Ma, M. D. Dickey, and J. J. Adams, "Planar, multifunctional 3D printed antennas using liquid metal parasitics," *IEEE Access*, vol. 7, pp. 134245–134255, 2019.

[10] C. Borda-Fortuny, L. Cai, K. F. Tong, and K.-K. Wong, "Low-cost 3D-printed coupling-fed frequency agile fluidic monopole antenna system," *IEEE Access,* vol. 7, pp. 95058–95064, 2019.

[11] C. Wang, J. C. Yeo, H. Chu, C. T. Lim, and Y.-X. Guo, "Design of a reconfigurable patch antenna using the movement of liquid metal," *IEEE Antennas Wireless Propag. Lett.*, vol. 17, no. 6, pp. 974–977, Jun. 2018.

[12] L. Song, W. Gao, C. O. Chui, and Y. Rahmat-Samii, "Wideband frequency reconfigurable patch antenna with switchable slots based on liquid metal and 3-D printed microfluidics," *IEEE Trans. Antennas Propag.*, vol. 67, no. 5, pp. 2886–2895, May 2019.

[13] K. Y. Alqurashi *et al.*, "Liquid metal bandwidth-reconfigurable antenna," *IEEE Antennas Wireless Propag. Lett.*, vol. 19, no. 1, pp. 218–222, Jan. 2020.

[14] A. Dey, R. Guldiken, and G. Mumcu, "Microfluidically reconfigured wideband frequency-tunable liquid-metal monopole antenna," *IEEE Trans. Antennas Propag.*, vol. 64, no. 6, pp. 2572–2576, Jun. 2016.

[15] X. Bai, M. Su, Y. Liu, and Y. Wu, "Wideband pattern-reconfigurable cone antenna employing liquid-metal reflectors," *IEEE Antennas Wireless Propag. Lett.*, vol. 17, no. 5, pp. 916–919, May 2018.

[16] R. Goteti, R. Jackson, and R. Ramadoss, "MEMS-based frequency switchable microstrip patch antenna fabricated using printed circuit processing techniques," *IEEE Antennas Wireless Propag. Lett.*, vol. 5, pp. 228–230, 2006.

[17] W. Baek *et al.*, "A V-band micromachined 2-D beam steering antenna driven by magnetic force with polymer-based hinges," *IEEE Trans. Microw. Theory Techn.,* vol. 51, no. 1, pp. 325–331, Jan. 2003.

[18] C. Wang, J. C. Yeo, H. Chu, C. T. Lim, and Y.-X. Guo, "Design of a reconfigurable patch antenna using the movement of liquid metal," *IEEE Antennas Wireless Propag. Lett.*, vol. 17, no. 6, pp. 974–977, Jun. 2018.

[19] S. Hage-Ali *et al.*, "A millimeter-wave microstrip antenna array on ultra-flexible micromachined polydimethylsiloxane (PDMS) polymer," *IEEE Antennas Wireless Propag. Lett.*, vol. 8, pp. 1306–1309, 2009.

[20] Y. Yang and Z. D. Deng, "Stretchable sensors for environmental monitoring," *Appl. Phys. Rev.,* vol. 6, no. 1, Mar. 2019, Art. no. 011309.

[21] Q.-Y. Tang, Y.-M. Pan, Y. C. Chan, and K. W. Leung, "Frequency-tunable soft composite antennas for wireless sensing," *Sensors Actuators A, Phys.,* vol. 179, pp. 137–145, Mar. 2012.

[22] X. J. Jiang, S. Jalali Mazlouman, A. Mahanfar, R. G. Vaughan, and C. Menon, "DEA deformed stretchable patch antenna," *Smart Mater. Struct.,* vol. 21, no. 5, May 2012, Art. no. 055020.

[23] M. Cosker, L. Lizzi, F. Ferrero, R. Staraj, and J.-M. Ribero, "Realization of 3-D flexible antennas using liquid metal and additive printing technologies," *IEEE Antennas Wireless Propag. Lett.*, vol. 16, pp. 971–974, 2017.

[24] P. Liu, S. Yang, X. Wang, M. Yang, J. Song, and L. Dong, "Directivity-reconfigurable wideband two-arm spiral antenna," *IEEE Antennas Wireless Propag. Lett.*, vol. 16, pp. 66–69, 2017.

[25] H. Moghadas, M. Zandvakili, D. Sameoto, and P. Mousavi, "Beam-reconfigurable aperture antenna by stretching or reshaping of a flexible surface," *IEEE Antennas Wireless Propag. Lett.*, vol. 16, pp. 1337–1340, 2017.

[26] H. Yagi, "Beam transmission of ultra short waves," *Proc. IEEE*, vol. 85, no. 11, pp. 1864–1874, Nov. 1997.